

1 **The p7 protein of the hepatitis C virus induces cell death differently from the influenza**  
2 **A virus viroporin M2.**

3

4 Jude Juventus Aweya<sup>a</sup>, Tze Minn Mak<sup>b</sup>, Seng Gee Lim<sup>c</sup> and Yee-Joo Tan <sup>a, b, d,\*</sup>

5 <sup>a</sup>Department of Microbiology and <sup>c</sup>Department of Medicine, Yong Loo Lin School of  
6 Medicine, National University Health System (NUHS), National University of Singapore,  
7 <sup>b</sup>NUHS Graduate School for Integrative Sciences and Engineering, Singapore, National  
8 University of Singapore, <sup>d</sup>Institute of Molecular and Cell Biology, A\*STAR (Agency for  
9 Science, Technology and Research), Singapore.

10

11

12 \*Correspondence to:

13 Address: MD4, 5 Science Drive 2, Singapore 117597

14 E-mail: Yee\_Joo\_TAN@NUHS.edu.sg

15 Tel: (65) 65163692

16 Fax: (65) 67766872

17

**18 Abstract**

19 Most viruses encode proteins that modulate cell-death signaling by the host. For hepatitis C  
20 virus (HCV) infection, apoptosis and other forms of cell-death have been observed in vitro  
21 and in vivo but the detailed understanding of this intricate viral-host interplay is unclear. This  
22 study examined the role played by the HCV p7 protein in the induction of cell-death. By  
23 measuring caspase-3/7 activation and cleavage of endogenous PARP, two hallmarks of  
24 apoptosis, the overexpression of p7 protein was shown to induce apoptosis in Huh7.5 cells.  
25 Furthermore, p7-induced apoptosis is caspase-dependent and involves both the intrinsic and  
26 extrinsic pathways. Similar to the M2 protein of influenza A virus, p7-induced apoptosis is  
27 independent of its ion channel activity. Coimmunoprecipitation experiments further showed  
28 that both M2 and p7 interact with the essential autophagy protein Beclin-1. However, only  
29 the M2 protein could cause an increase in the level of LC3-II, which is an indicator of  
30 autophagic activity. Thus, although the p7 protein is functionally similar to the well-  
31 characterized M2 protein, they differ in their activation of autophagic cell-death. Taken  
32 together, these results shed more light on the relationship between the HCV p7 ion channel  
33 protein and cell-death induction in host cells.

34

35 **Keywords:** HCV, p7 protein, cell death, ion channel activity

36

## 37 **1. Introduction**

38 Hepatitis C virus (HCV), a small positive strand RNA virus that belongs to the  
39 *Hepacivirus* genus in the *Flaviviridae* family, is one of the major causes of liver disease such  
40 as cirrhosis, steatosis, and hepatocellular carcinoma (Chen and Morgan, 2006). In fact, HCV  
41 infection is the most frequent indication for liver transplantation in developed countries  
42 (Brown, 2005). Currently, about 130 - 170 million or 3 % of the world population are  
43 estimated to be infected with HCV; with about 3 to 4 million new infections per year (WHO,  
44 2012). HCV has a high degree of genetic diversity, so it is classified phylogenetically into six  
45 major genotypes and several subtypes (Simmonds, 2004). The HCV genome of ~9.6 kb  
46 encodes a unique open reading frame that is translated into a precursor polyprotein of ~3000  
47 residues. Co- and post-translational processing of the polyprotein by both viral and cellular  
48 proteases yields three structural (Core, E1 and E2), six non-structural proteins (NS2-NS5),  
49 and a small membrane ion channel protein (p7) (Lin et al., 1994); the protein of interest in  
50 this study.

51 The HCV p7 protein, a small (63 amino acid) hydrophobic protein located between  
52 the structural and nonstructural region of HCV, is not clearly identified as structural or  
53 nonstructural protein, although it has been shown to be a transmembrane protein (reviewed in  
54 (Khaliq et al., 2011)). HCV p7 is classified as a viroporin, a group of small hydrophobic  
55 proteins encoded by a variety of RNA viruses that oligomerize to form pores (ion channels)  
56 in host-cell membranes through which viruses can enter/exit as well as contribute to virus  
57 assembly and pathology of disease by altering membrane permeability and disrupting ion  
58 homeostasis in cells (Gonzalez and Carrasco, 2003). The precise role of p7 in the HCV life-  
59 cycle has been hard to define. However, some recent papers have implicated p7 in the  
60 assembly and release of virus particles, mostly acting in concert with other viral proteins  
61 (reviewed in (Khaliq et al., 2011; Steinmann and Pietschmann, 2010)), and in a genotype-

62 specific manner (Steinmann et al., 2007). For example, a strain-specific tripartite relationship  
63 between core, p7 and NS2 has been reported to be responsible for modulating the subcellular  
64 localization of core (Boson et al., 2011) and NS2 (Tedbury et al., 2011), which is independent  
65 of p7's ion channel activity. Similarly, it has been shown that mutations in the p7 protein,  
66 either singly or in combination with E2 glycoprotein enhances several-fold production of  
67 infectious virus particles in cell culture (Kim et al., 2011). Thus, p7 unlike other viroporins  
68 such as M2 of influenza A virus and Vpu of HIV-1, is absolutely essential for HCV  
69 replication in vitro (Brohm et al., 2009; Steinmann et al., 2007).

70 Cell death regulation is an important determinant in the survival of most viruses,  
71 therefore, many viruses encode proteins that interfere with cell death signaling pathways,  
72 skewing it in their favour (Chen et al., 2006). For HCV, both proapoptotic and prosurvival  
73 properties have been attributed to different HCV proteins (reviewed in (Aweya and Tan, 2011;  
74 Fischer et al., 2007)). HCV p7 like other members of the viroporins (e.g., HIV-1 Vpu, human  
75 T-cell lymphotropic virus-1 p13II, hepatitis B virus X protein, and influenza virus PB1  
76 ORF2), might be targeted to the mitochondrial membranes where it modulates apoptosis by  
77 altering the mitochondrial membrane permeability. However, there is currently limited  
78 information on the apoptotic activity of p7 except that reported by Madan *et al* (Madan et al.,  
79 2008) who demonstrated that the p7 protein of genotype 1b HCV induces caspase-dependent  
80 apoptosis via the mitochondria in baby hamster kidney cells. Since the genotype 2a JFH1  
81 strain is the only one that can replicate efficiently in permissive cells, such as Huh7.5 cells,  
82 without adaption, this study sought to examine how p7 protein of this strain modulates cell-  
83 death and how similar it is to the M2 ion channel protein of influenza A virus, which is a well  
84 characterized viroporin. We were able to show that HCV p7 protein induces caspase-  
85 dependent apoptosis which is independent of its ion channel activity, and although p7 protein

86 shares a couple of functional properties with M2 protein of influenza A virus, they seem to  
87 differ in their induction of autophagic cell death.

88

89

## 90 **2. Materials and Methods**

### 91 *2.1. Cell culture and cell lines*

92 Huh7.5 cells (subclone of the Huh-7 human hepatoma cell line; Apath, Brooklyn,  
93 NY) and 293FT cells (human embryonic kidney cell line with the temperature sensitive gene  
94 for SV40 T-antigen; Invitrogen, Karlsruhe, Germany) were grown in Dulbecco's modified  
95 Eagle's medium (Invitrogen) supplemented with 10 % fetal bovine serum (HyClone, Utah,  
96 USA), nonessential amino acids and antibiotics (10 units/ml penicillin and 10 µg/ml  
97 streptomycin) (Invitrogen, Carlsbad, CA). All cells were maintained in a 37 °C incubator  
98 with 5 % CO<sub>2</sub>.

99

### 100 *2.2. Plasmid Construction*

101 Expression plasmids for the HCV p7 proteins were generated by PCR cloning using  
102 Titanium Taq DNA polymerase (Clontech Laboratories Inc., Palo Alto, CA). Two plasmids  
103 containing the full-length HCV genome of the genotype 1b (S1) cloned in Singapore ((Soo et  
104 al., 2002) GenBank accession number AF356827) and genotype 2a JFH-1 strain (Wakita et  
105 al., 2005), GenBank accession number AB047639) were used as templates. The PCR  
106 products were digested with restriction enzymes BamHI and XhoI and then ligated into the  
107 pXJ40flag vector which is a flag-tagged plasmid derived from pXJ40 (Xiao et al., 1991). The  
108 pXJ40flag vector was used so that a flag epitope is fused to the N-terminus of the p7 protein  
109 to allow the comparison of protein expression levels with an anti-flag antibody. Similarly, the  
110 p7 mutants were generated by 2 rounds of PCR: the first round of PCR was used to generate  
111 5' and 3' fragments of p7 containing the appropriate alanine or glutamine substitutions; these  
112 were then amplified into full-length p7 using end primers for the p7 gene and cloned into  
113 pXJ40flag vector using BamHI and XhoI sites. The M2 gene of influenza A virus (A/Puerto  
114 Rico/8/34/Mount Sinai/Wi (H1N1), GenBank accession number AY768951.1) was produced

115 by gene synthesis (GenScript USA Inc Piscataway, NJ, USA) and cloned into the pXJ40flag  
116 vector in a similar manner. All sequences were confirmed by sequencing performed by the  
117 DNA Sequencing Facility at the Department of Microbiology, Yong Loo Lin School of  
118 Medicine, National University of Singapore, Singapore.

119

### 120 *2.3. Transient transfections and Western blot analysis*

121 Transient transfections of cells were performed using Lipofectamine 2000 reagent  
122 (Invitrogen, Carlsbad, CA) according to the manufacturer's protocol. Approximately 24 h  
123 after transfection, the cells were harvested by scrapping into the media, spun down in a  
124 bench-top centrifuge and washed twice with cold PBS. The cell pellets were then  
125 resuspended in RIPA buffer (50 mM Tris (pH 8.0), 150 mM NaCl, 0.5 % NP40, 0.5 %  
126 deoxycholic acid, 0.005 % SDS and 1 mM phenylmethylsulfonyl fluoride) and subjected to  
127 freeze-thawing five times before being spun down at 13000 rpm to remove cellular debris.  
128 The cell lysate was then used for Western blot analysis and quantification of apoptosis (see  
129 next section below).

130 Primary antibodies used in the study included anti-actin monoclonal, anti-flag  
131 monoclonal and polyclonal (Sigma, St. Louis, MO), anti-poly [ADP-ribose] polymerase  
132 [PARP] polyclonal, and anti-LC3B polyclonal (Cell Signaling Technology Inc., Beverly, MA)  
133 antibodies. Secondary antibodies used included horseradish peroxidase (HRP)-conjugated  
134 goat anti-mouse, and goat anti-rabbit antibodies (Pierce, Rockford, IL).

135

### 136 *2.4. Apo-One fluorometric and TUNEL assay*

137 Apoptosis was quantified in the form of caspase-3/7 activation using the Apo-One  
138 fluorometric assay system from Promega Corporation (Madison, WI) according to the  
139 manufacturer's protocol. To further confirm the induction of apoptosis by cells

140 overexpressing p7 protein, the Terminal deoxynucleotidyl transferase dUTP nick end labeling  
141 (TUNEL) assay was carried out after 24 h of transfection using the DeadEnd Fluorometric  
142 TUNEL system (Promega, Madison, WI) according to the manufacturer's protocol. Briefly,  
143 cells were plated in Lab-Tek™ Chamber Slides, transfected with plasmids expressing p7  
144 protein followed by treatment with cell permeable caspase inhibitors as described below.  
145 After 24 h, cells were fixed in 4% paraformaldehyde at 4°C for 25 min. Fixed cells were then  
146 permeabilized in 0.2% Triton X-100 and labelled with fluorescein-12-dUTP using terminal  
147 deoxynucleotidyl transferase. After rinsing with PBS, slides were mounted with  
148 VECTASHIELD® Mounting Medium with DAPI (Vector Laboratories, Burlingame, CA).  
149 The TUNEL-positive cells (green fluorescence) corresponding to the nuclei location (DAPI)  
150 were captured with Olympus FluoView FV1000 (Olympus, Japan) laser scanning confocal  
151 microscope using a 60x/1.45 oil objective, with 543nm HeNe laser as the excitation source.

152

### 153 *2.5. Treatment of cells with caspase inhibitors and ammonium chloride*

154 Cells were transfected (as above) followed by treatment with 2.5 µM of caspase-3 (Z-  
155 DEVD-fmk), caspase-8 (Z-IETD-fmk), caspase-9 (Z-LEHD-fmk) or a negative caspase  
156 inhibitor (Z-FA-fmk) (BD Biosciences). Briefly, 6 h post-transfection, the transfection media  
157 was changed and replenished with fresh media plus 2.5 µM of the respective cell permeable  
158 caspase inhibitors which are reported to have a very short half-life (Ekert et al., 1999; Garcia-  
159 Calvo et al., 1998). After about 24 h post-transfection, the cells were harvested by scrapping  
160 into the media, spun down in a bench-top centrifuge and washed three times with 1X cold  
161 PBS to remove any residual inhibitor found in the media. The cell pellets were then  
162 resuspended in RIPA buffer and subjected to freeze-thawing five times before being spun  
163 down at 13000 rpm to clarify the lysate. Subsequently, the lysate was analysed using the  
164 Apo-One fluorometric assay as described above.



165 In order to block autophagosome formation, cells were treated with ammonium  
166 chloride (BDH, AnalaR). Briefly, the spent media from an overnight transient transfection  
167 was replaced with complete media containing 2.7 mg/ml of ammonium chloride and then  
168 incubated further for 2.5 h. Cells were then washed twice with 1X cold PBS, lysed directly in  
169 2X Laemmli's sodium dodecyl sulfate (SDS) buffer and the cell lysate subjected to SDS-  
170 polyacrylamide gel electrophoresis, followed by Western blot analysis to determine the  
171 conversion of LC3-I to LC3-II.

172

### 173 *2.6. Coimmunoprecipitation experiments*

174 For the coimmunoprecipitation experiments, each 6 cm dish of cells was resuspended  
175 in 400  $\mu$ l of RIPA buffer and subjected to freeze-thawing five times. Anti-Beclin-1 rabbit  
176 polyclonal antibody (Santa Cruz Biotechnology, Santa Cruz, CA) was added to the lysates  
177 containing 200  $\mu$ g of total protein and allowed to mix for 1 h at 4 °C. Protein A agarose beads  
178 (Roche, Indianapolis, IN) were added, and the mixture was subjected to end-over-end mixing  
179 at 4 °C overnight. Beads were washed four times with cold RIPA buffer, and then 15  $\mu$ l of  
180 Laemmli's SDS buffer was added and the samples were boiled at 100 °C for 5 min to release  
181 the immunocomplexes. Samples were separated by SDS-polyacrylamide gel electrophoresis  
182 and subjected to Western blot analysis as described above.

183

### 184 *2.7. Membrane permeabilization assay*

185 Permeability of the plasma membrane of cells expressing p7 or mutants to  
186 hygromycin B (a translation inhibitor) was a modification of the method described by Liao *et*  
187 *al* (Liao et al., 2006). Briefly, 293FT cells in 6 cm dishes were transfected with plasmids as  
188 described above, followed by treatment of the cells with different concentrations of  
189 hygromycin B (Roche) for 30 min at 6 h post-transfection. After 24 h post-transfection, the

190 cells were harvested, lysed in RIPA buffer and subjected to freeze-thaw five times. The cell  
191 extracts were then spun at 13,000 rpm for 20 min at 4 °C to clarify the lysate. The proteins  
192 were immunoprecipitated with anti-Flag beads (Sigma) overnight at 4 °C, and washed three  
193 times with RIPA buffer. The samples were then analyzed by 15% SDS-PAGE.

194

### 195 *2.8. Immunofluorescence assay*

196 For indirect immunofluorescence staining, transfected Huh 7.5 cells grown on coverslips  
197 were fixed with 4 % paraformaldehyde in PBS for 15 min. Fixed cells were permeabilized  
198 with 0.2% Triton X-100 in PBS for 5 min, blocked with 1 % bovine serum albumin (BSA) in  
199 PBS for 30 min and incubated with primary antibodies (anti-flag polyclonal (Sigma)) for 1 h.  
200 After washing, cells were incubated with Alexa-Fluor-564-conjugated goat anti-rabbit IgG  
201 secondary antibodies (Invitrogen) for 1 h. Images were captured with Olympus BX60  
202 fluorescence microscope (Olympus, Japan) using a 100x oil objective.

203

### 204 *2.9. Quantification of autoradiographs and statistical analysis*

205 ImageJ open-source gel analysis software (Rasband) was used for the quantification  
206 of the intensities of specific bands on autoradiographs. All experiments were repeated at least  
207 three times. The mean data is presented. Statistical analysis was performed using the  
208 Student's t-test.  $p < 0.05$  was considered significant.

209

### 210 **3. Results**

#### 211 *3.1. HCV p7 protein induces apoptosis in Huh7.5 cells*

212 To determine if genotype 2a HCV p7 protein can induce apoptosis in host cells,  
213 Huh7.5 cells, which are highly permissive for HCV replication, were transiently transfected  
214 with a cDNA expression plasmid containing the genotype 2a (JFH-1 strain) p7. For  
215 comparison, Huh7.5 cells were also transfected with genotype 1b (S1) HCV p7 protein, the  
216 empty vector or an expression plasmid containing the Bax gene, which is a well-known  
217 apoptosis inducer that acts via the mitochondria. About 24 h post-transfection, the cells were  
218 harvested, lysed and the cell lysate was used for western blot analysis and measurement of  
219 the activation of caspase-3/7, which is a hallmark of apoptosis. As shown in Fig.1A, cells  
220 overexpressing genotype 1b p7 (abbreviated p7-1b), genotype 2a p7 (abbreviated p7-2a), or  
221 Bax have significantly higher level of caspase-3/7 activity than the vector control cells.  
222 Similarly, the cleavage of endogenous poly (ADP-ribose) polymerase (PARP), a substrate of  
223 activated caspase-3/7, was clearly observed in cells overexpressing p7-1b, p7-2a and Bax but  
224 there was less cleavage in cells transfected with the empty vector (Fig. 1B, middle). Western  
225 blot analysis showed the expression of flag-tagged protein (Fig. 1B, top) and endogenous  
226 actin (Fig. 1B, bottom). The rest of the experiments were performed using only the genotype  
227 2a p7 (hereafter p7).

228

#### 229 *3.2. HCV p7-induced apoptosis is caspase-dependent*

230 To determine if p7-induced apoptosis is caspase-dependent, Huh7.5 cells were  
231 transiently transfected with the p7 plasmid, followed by treatment with cell permeable pan-  
232 caspase inhibitor (zVAD-fmk) or an irrelevant peptide (zFA-fmk) 6 h post-transfection. The  
233 level of apoptosis induced, as measured by caspase-3/7 activity, was observed to be  
234 significantly inhibited by the pan-caspase inhibitor but not the irrelevant peptide, suggesting

235 the involvement of a caspase-dependent pathway in p7-induced apoptosis (Fig. 2A).  
236 Consistently, there was only a low level of cleaved PARP, as detected by western blot  
237 analysis, in the p7-overexpressing cells treated with zVAD-fmk treated cells (Fig. 2B,  
238 middle). However, a high level of cleaved PARP was observed in the p7-overexpressing  
239 cells that were treated with zFA-fmk (Fig. 2A, densitometry values below). To confirm the  
240 involvement of caspases in p7-induced apoptosis, the terminal uridine nick 3' end-labeling  
241 (TUNEL) assay was performed. Cells overexpressing p7 and treated with the irrelevant  
242 peptide (zFA-fmk) had more TUNEL-positive cells than those treated with the pan-caspase  
243 inhibitor (zVAD-fmk) (Fig. 4, top right panel).

244

### 245 *3.3. HCV p7 protein induces apoptosis via both the intrinsic and extrinsic pathways*

246 Since p7 induces apoptosis via caspase-dependent pathway, the next step was to  
247 determine which of the caspase-dependent pathways are involved. To examine this, cell  
248 permeable non-toxic peptide caspase inhibitors that bind irreversibly to activated caspases  
249 and which have a short half-life (Ekert et al., 1999; Garcia-Calvo et al., 1998) and specific for  
250 different caspases, namely caspase-3 (zDEVD-fmk), caspase-8 (zIETD-fmk) and caspase-9  
251 (zLEHD-fmk), were added to the cells 6 h post-transfection. As shown in Fig. 3A, the level  
252 of p7-induced apoptosis after about 24 h post-transfection, as reflected by the caspase-3/7  
253 activity in the cell lysate, was significantly inhibited by all three caspase inhibitors, but not by  
254 the irrelevant peptide (zFA-fmk). However, high levels of cleaved PARP were still observed  
255 in cells treated with the caspase inhibitors despite the low caspase-3/7 activity (Fig. 3B,  
256 middle). This could possibly be due to the cleavage of PARP by caspase-independent events  
257 (Yang et al., 2004) and other caspases in the absence of caspase-3 or caspase-7 activation.  
258 Indeed, it has been reported that PARP can be cleaved by other proteases and protease-like  
259 molecules as well as several caspases (Fernandes-Alnemri et al., 1995; Germain et al., 1999;

260 Lippke et al., 1996; Malireddi et al., 2010; Muzio et al., 1996; Orth et al., 1996; Tewari et al.,  
261 1995) albeit at lower efficiency than by caspase-3 or -7. Similarly, the number of TUNEL-  
262 positive cells was not much different between cells treated with the irrelevant peptide (zFA-  
263 fmk) and the three caspase inhibitors (Fig. 4, lower panel). One could therefore speculate that,  
264 probably because p7-induced PARP cleavage and DNA fragmentation are late apoptosis  
265 events (Collins et al., 1997; Duriez and Shah, 1997), they could not be completely blocked  
266 when a caspase inhibitor that is specific for only one of the caspases is used. Nevertheless,  
267 our results showed that p7-induced apoptosis is indeed caspase-dependent and involves  
268 activation of both caspase-8 and -9 which are initiator caspases of the death receptor  
269 (extrinsic) and mitochondria-mediated (intrinsic) pathways respectively, and found upstream  
270 of caspase-3/7, the executioner caspases.

271

#### 272 *3.4. HCV p7-induced apoptosis does not depend on its ion channel activity*

273 The HCV p7 protein possesses ion channel activity and is thus classified in the family  
274 of viral ion channel proteins known as viroporins (Griffin et al., 2003; Pavlovic et al., 2003).  
275 Moreover, H17, located within the amino-terminal transmembrane domain of p7, has been  
276 implicated in p7's ion channel function, and has also been shown to share functional  
277 similarity with H37 of the influenza A virus M2 ion channel protein (StGelais et al., 2009).  
278 However, the p7 of genotype 2a has an additional H31, which is found in only a few other  
279 genotypes and thought to partly influence the gating function of p7 (Brohm et al., 2009;  
280 Montserret et al., 2010). Thus, in order to express p7 lacking ion channel activity and to  
281 eliminate the probable influence of H31, both H17 and H31 were substituted with A to  
282 generate a double substitution mutant p7H17AH31A. Using the membrane permeabilization  
283 assay (see materials and methods section for details), the overexpression of p7 resulted in the  
284 permeabilization of the cell membrane, as the translation of p7 protein was clearly inhibited

285 in the presence of Hygromycin B (Fig. 5A, left panel). In contrast, the overexpression of  
286 p7H17AH31A seems to have little effect on membrane permeability as the addition of  
287 Hygromycin B did not inhibit the translation of p7H17AH31A to a great extent (Fig. 5A,  
288 right panel).

289 When the level of apoptosis of cells overexpressing p7 and the double mutant was  
290 subsequently measured, it was observed that both the wild-type p7 protein and the  
291 p7H17AH31A mutant induced significantly higher caspase-3/7 activity than the vector (Fig.  
292 5B). It therefore appears that p7-induced apoptosis is independent of its ion channel activity.  
293 In addition, the cleavage of endogenous PARP, a substrate of activated caspase-3/7, was  
294 clearly observed in Huh7.5 cells overexpressing either the wild-type p7 protein or the  
295 p7H17AH31A mutant (Fig. 5C, middle).

296

### 297 *3.5. Mutation of the conserved dibasic amino acids in the cytoplasmic domain of p7 protein* 298 *affects its apoptosis activity*

299 Apart from the histidine residues in p7, there are two highly conserved basic amino  
300 acids (K/R33 and R35) in the cytoplasmic domain of p7 protein. When these dibasic residues  
301 in p7 are substituted by A or Q, the ion channel activity of p7 is lost and the production of  
302 infectious particles is reduced (Griffin et al., 2004; Steinmann et al., 2007). To determine if  
303 these amino acid residues are essential for the apoptotic activity of p7 protein, substitution  
304 mutants were generated in the background of genotype 2a HCV p7 protein. Using the  
305 membrane permeabilization assay, we demonstrated that these mutants lacked ion channel  
306 activity (results not shown). However, compared to the wild-type p7 protein, overexpression  
307 of the mutants had a significantly lower level of caspase-3/7 activity (Fig. 6A). Both single  
308 and double substitution mutants were expressed at higher levels than the wild-type p7 protein,  
309 indicating that the lack of apoptosis is not a consequence of lower protein expression levels

310 (Fig. 6B, top). As it has been reported that these residues (R33 and R35) are important in  
311 maintaining the topology of p7 (Steinmann et al., 2007), the mutants could not induce much  
312 apoptosis as the wild-type p7 probably because they are orientated wrongly in the host  
313 membranes.

314

### 315 *3.6. HCV p7 protein does not induce autophagic cell death but can interact with Beclin-1*

316 Based on the above characterization of p7, it seems that p7, like M2 protein, can  
317 induce caspase-dependent apoptosis, but this is independent of ion channel activity. M2 has  
318 also been shown to block autophagosome fusion with lysosomes and resulting in cell death  
319 (Gannage et al., 2009). Thus, to examine if p7 protein behaves in the same manner as M2,  
320 Huh7.5 cells were transfected with plasmids for expressing p7 and M2 and their effects on  
321 the conversion of microtubule-associated protein 1 light chain 3 (LC3) from isomer I to  
322 isomer II (LC3-I to LC3-II) was analysed using western blot. However, M2 failed to block  
323 macroautophagy probably due to the low transfection efficiency in Huh7.5 cells (data not  
324 shown). Hence, the experiment was repeated using the highly transfectable 293FT cells  
325 (Invitrogen) which is derived from human embryonal kidney cells transformed with the SV40  
326 large T antigen to allow very high levels of protein expression from vectors containing the  
327 SV40 origin (<http://products.invitrogen.com/ivgn/product/R70007>). The results showed that  
328 both p7 and M2 induce apoptosis in 293FT cells when overexpressed (Fig. 7A and B), which  
329 is consistent with p7 induction of apoptosis in Huh7.5 cells (see above) and M2 in BHK cells  
330 (Madan et al., 2008). Interestingly, the levels of activated caspase-3/7 as well as cleaved  
331 PARP were much higher in the cells over-expressing p7 compared to those over-expressing  
332 M2. In lane 2, the major band for M2 is ~ 20 kDa, which is the expected molecular weight,  
333 but there are also some higher molecular weight bands. These are likely to be oligomers of  
334 M2 which are resistant to boiling, 20 mM dithiothreitol, and 1% SDS (which are found in the

335 Laemmli SDS loading buffer) as we have previously observed the same phenomenon with  
336 another transmembrane protein (Tan et al., 2007).

337 Consistent with the previous study (Gannage et al., 2009), the level of LC3-II in M2  
338 overexpressing cells was much higher than cells transfected with the empty vector (Fig. 8A  
339 (middle), lanes 2 and 4). After performing four independent experiments and using  
340 densitometry to quantify the intensities of LC3-I and II, the conversion to LC3-II (i.e. LC3-  
341 II/LC3-I+LC3-II) was found to be significantly higher (63%) in the cells overexpressing M2  
342 as compared to the cells transfected with the empty vector (49%). In contrast, the level of  
343 LC3-II (the autophagic marker) in p7 overexpressing cells (41%) was not significantly  
344 different from the cells transfected with the empty vector (Fig. 8B). Untransfected cells  
345 untreated and treated with ammonium chloride, which is an inhibitor of autophagosome  
346 formation, served as negative and positive controls respectively. As the percentage of  
347 conversion to LC-II in the M2 overexpressing cells (63%) was statistically significant as in  
348 the case of the ammonium chloride-treated cells (87%), the assay was deemed sensitive  
349 enough to detect autophagic cell death. The expression of flag-tagged protein was detected by  
350 Western blot analysis (Fig. 8A, top) and the level of endogenous actin (Fig. 8A, bottom) was  
351 used as the loading control of the total proteins in the cell lysates. In addition to LC3-II as an  
352 autophagosome marker, we also analyzed the accumulation of GFP-LC3 puncta (Bampton et  
353 al., 2005; Mizushima, 2009). Huh7.5 cells were transiently transfected with GFP-LC3 and  
354 M2 or p7 expression plasmids. Twenty-four hours post transfection; we observed that only  
355 cells overexpressing M2 and GFP-LC3 showed an increased accumulation of LC3 puncta by  
356 immunofluorescence microscopy analysis (Fig. 9A).

357 To further examine the difference in the ability of p7 and M2 to induce autophagic  
358 cell death, co-immunoprecipitation experiment was next performed to determine if they can  
359 interact with Beclin-1, which is a key component of the molecular machinery of



360 macroautophagy (reviewed in (Kang et al., 2011)) and also constitutes a major target for  
361 manipulation of autophagy by viruses (Dai et al., 2012; Munz, 2011). As shown in in the top  
362 panel of Figure 9B, both flag-M2 and flag-p7, but not by an irrelevant protein, glutathione *S*-  
363 transferase (GST), bound to the endogenous Beclin-1 protein. The expression levels of the  
364 flag-tagged proteins in the cell lysates were similar (Fig. 9B, middle) and endogenous Beclin-  
365 1 expression was not affected by the expression of the flagged tag proteins (Fig. 9B, bottom).  
366 Hence, it appears that the binding of p7 to Beclin-1 is not sufficient to interfere with the  
367 autophagic process.

368

369

370

#### 371 4. Discussion

372           Currently, apoptosis or caspase-dependent cell death is the most well characterized  
373 cell death pathway, although there is increasing evidence that other non-apoptotic or caspase-  
374 independent cell death pathways are involved in programmed cell death (Hetz et al., 2005).  
375 Autophagic cell death and programmed necrosis (necroptosis) are cell death mechanisms  
376 which are also important in viral infections and are thought to be exploited by viruses for  
377 their survival (Edinger and Thompson, 2004; Park et al., 2012). There is also some crosstalk  
378 or interrelationship between the different cell death mechanisms which is exploited by some  
379 viruses for their survival in the host, as reported for influenza A virus which determines the  
380 death of its host by inducing apoptosis and blocking autophagy (Gannage et al., 2009). With  
381 some recent studies suggesting that HCV induces caspase-independent cell death such as  
382 autophagy (reviewed in (Dreux and Chisari, 2011)), it is possible that HCV, like influenza A  
383 virus, might also be exploiting the interrelationship between apoptosis and non-apoptotic cell  
384 death for its survival in the host. Incidentally, the protein of interest in this study, p7 protein,  
385 happens to share some functional relationship with influenza A virus M2 protein (Mihm et al.,  
386 2006), so it is tempting to speculate that p7 and M2 might play similar roles in cell death  
387 modulation.

388           Currently, the apoptotic activity of p7 of different HCV genotypes have not been  
389 reported except that of genotype 1b (Madan et al., 2008). Since the genotype 2a JFH1 strain  
390 is the only one that can replicate efficiently in permissive cells, such as Huh7.5 cells, without  
391 adaption, this study focuses on characterizing the cell death pathways activated by the p7  
392 protein of the JFH-1 strain. To our knowledge, this is the first time that the p7 protein of  
393 genotype 2a has been shown to induce apoptosis to a similar level as that of genotype 1b p7  
394 (Fig. 1). As for genotype 1b p7, the result is similar to the observation by Madan *et al*  
395 (Madan et al., 2008b) except that Huh7.5 cells were used in this study while BHK cells were

396 used in the previous study. Further characterization of the apoptosis induced by the p7 protein  
397 of genotype 2a reveals that p7-induced apoptosis was efficiently blocked by a pan-caspase  
398 inhibitor as well as inhibitors specific for caspases 3, 8 or 9 (Fig. 2 and 3). In mammalian  
399 cells, apoptosis can be induced via two major pathways; the death receptor pathway (extrinsic  
400 pathway), triggered by the binding of FasL to Fas (CD95), with caspase-8 as the initiator  
401 caspase; and the mitochondria-mediated pathway (intrinsic pathway), induced by the  
402 mitochondria in response to DNA damage, oxidative stress and viral proteins, with caspase-9  
403 as the initiator caspase(Kumar, 2007). Thus, our results confirm that p7-induced apoptosis is  
404 indeed caspase-dependent and involves both the intrinsic and extrinsic apoptosis pathways.

405         Given that some previous studies have reported that ions channels play a key role in  
406 the regulation of cell physiology and in the induction of apoptotic cell death (Burg et al.,  
407 2006; Lang et al., 2003; Szabo et al., 2004), it was important to also determine whether this  
408 property of p7 has a link with its apoptotic activity. Although, details and the exact function  
409 of most ion channels in apoptosis mediation are currently unknown, it is believed that some  
410 viruses employ the control of ion channel homeostasis to promote viral persistence  
411 (Mankouri et al., 2009). A recent study has demonstrated a relationship between ion channel  
412 activity and apoptosis by showing that the caspase-dependent apoptosis induced by the  
413 SARS-coronavirus 3a protein (which possesses ion channel activity) is abolished when its ion  
414 channel activity is blocked (Chan et al., 2009). In the case of p7, substitution of the two  
415 histidine residues (H17 and H31), which have been implicated in the gating function of p7  
416 (Brohm et al., 2009; Montserret et al., 2010), with alanine, did not reduce its apoptotic  
417 activity greatly (Fig. 5B), although the resultant double mutant had lost most of its ion  
418 channel activity (Fig. 5A). It thus suggests that the caspase-dependent apoptosis induced by  
419 p7 protein is independent of its ion channel function. Nevertheless, p7 has to be properly  
420 folded and maintain the correct topology in the cell membranes in order to induce apoptosis

421 as single or double substitution of the dibasic amino acid residues R33 and R35, to glutamine  
422 (Q) in the background of genotype 2a HCV p7 protein significantly reduced the level of  
423 apoptosis induced by p7 (Fig. 6) and to function as an ion channel. This observation is in line  
424 with a previous report that mutating the dibasic motif of p7 can substantially impact on the  
425 polyprotein processing and thus distort the topology of p7 protein (Steinmann et al., 2007).

426         Recent studies (reviewed in (Eisenberg-Lerner et al., 2009; Gordy and He, 2012;  
427 Zhou et al., 2011)) have shown that there seems to exist a connection between pathways that  
428 regulate autophagy and apoptosis, with a number of molecules including Bcl-2 family  
429 proteins, Beclin-1, caspase-8, caspase-9, phosphoinositide-3-kinase class I, and ceramide  
430 implicated in the control of both apoptosis and autophagy. Apart from apoptotic or caspase-  
431 dependent cell death, HCV is reported to induce non-apoptotic cell death such as autophagy  
432 (reviewed in (Dreux and Chisari, 2011)). In one such report, when the autophagy machinery  
433 of HCV-infected hepatocytes was interrupted, it resulted in the induction of apoptosis  
434 (Shrivastava et al., 2011). Thus, it is believed that HCV exploits the autophagy pathway for  
435 its propagation and survival in the host, although the biological significance of this in the  
436 lifecycle HCV is still unclear (Taguwa et al., 2011). Similarly, the pro-apoptotic M2 ion  
437 channel protein of influenza A virus is reported to cause accumulation of autophagosomes by  
438 blocking their fusion with lysosomes which thus leads to apoptosis of the infected cells  
439 (Gannage et al., 2009). Since both p7 and M2 are viroporins and are known to induce  
440 caspase-dependent cell death, several experiments were therefore conducted to determine if  
441 the p7 protein behaves like M2 protein of influenza A virus. Our results showed that unlike  
442 M2, the overexpression of p7 did not significantly increase the conversion of LCI to LCII  
443 (Fig. 8) or the accumulation of GFP-LC3 puncta (Fig. 9A) suggesting that probably p7 was  
444 not involved in autophagosome maturation despite the fact that both flag-tagged M2 and p7  
445 could interact with endogenous Beclin-1 in co-immunoprecipitation experiment (Fig. 9B).

446 Since a number of viral proteins including M2 have been reported to interact with Beclin-1  
447 and thus interfere with the class III PI3K (UVRAG-Beclin-1-hVps34) complex's function in  
448 autophagosome maturation (Dai et al., 2012; He and Levine, 2010; Munz, 2011), it is  
449 therefore tempting to speculate that probably M2 and p7 bind to different domains in the  
450 class III PI3K complex, with only M2 able to interact with and inhibit autophagosome  
451 maturation (Gannage et al., 2010).

452 Taken together, these results indicate that HCV p7 protein induces caspase-dependent  
453 apoptosis which is independent of its ion channel activity. Although p7 and M2 share some  
454 functional properties in terms of ion channel and pro-apoptotic activity, they seem to differ in  
455 their abilities to induce autophagic cell death. Further studies are underway in our laboratory  
456 to identify residues or motifs that are responsible for the apoptosis activity of p7. The HCVcc  
457 system will then be used to generate mutant virus containing mutation(s) that abolishes p7  
458 pro-apoptotic activity and establish the functional significance of the apoptosis activity of p7  
459 during HCV infection. In addition, identification of these residues will allow the study of the  
460 interaction between HCV p7 and other viral and host factors in cell death signaling during an  
461 infection.

462

463

#### 464 **Acknowledgements**

465 We thank T. Wakita for the JFH-1 construct and Megha Haridas Upadya for technical  
466 assistance in the fluorescence and confocal microscopy work. This work was supported by a  
467 NUHS Cross Department Collaborative Grant [R-182-000-171-733] to S. G. Lim and Y.-J.  
468 Tan, and a NUS/NUHS start-up grant [R-182-000-156-720 and R-182-000-156-133] to Y.-J.  
469 Tan.

470

471 **References**

472

473 Aweya, J.J., Tan, Y.J., 2011. Modulation of programmed cell death pathways by the hepatitis  
474 C virus. *Front Biosci* 16, 608-618.

475 Bampton, E.T., Goemans, C.G., Niranjana, D., Mizushima, N., Tolkovsky, A.M., 2005. The  
476 dynamics of autophagy visualized in live cells: from autophagosome formation to fusion  
477 with endo/lysosomes. *Autophagy* 1(1), 23-36.

478 Boson, B., Granio, O., Bartenschlager, R., Cosset, F.L., 2011. A concerted action of hepatitis  
479 C virus p7 and nonstructural protein 2 regulates core localization at the endoplasmic  
480 reticulum and virus assembly. *PLoS Pathog* 7(7), e1002144.

481 Brohm, C., Steinmann, E., Friesland, M., Lorenz, I.C., Patel, A., Penin, F., Bartenschlager, R.,  
482 Pietschmann, T., 2009. Characterization of Determinants Important for Hepatitis C Virus  
483 p7 Function in Morphogenesis by Using trans-Complementation. *J Virol* 83(22), 11682-  
484 11693.

485 Brown, R.S., 2005. Hepatitis C and liver transplantation. *Nature* 436(7053), 973-978.

486 Burg, E.D., Remillard, C.V., Yuan, J.X., 2006. K<sup>+</sup> channels in apoptosis. *J Membr Biol*  
487 209(1), 3-20.

488 Chan, C.M., Tsoi, H., Chan, W.M., Zhai, S., Wong, C.O., Yao, X., Chan, W.Y., Tsui, S.K.,  
489 Chan, H.Y., 2009. The ion channel activity of the SARS-coronavirus 3a protein is linked  
490 to its pro-apoptotic function. *Int J Biochem Cell Biol* 41(11), 2232-2239.

491 Chen, S.L., Morgan, T.R., 2006. The natural history of hepatitis C virus (HCV) infection. *Int*  
492 *J Med Sci* 3(2), 47-52.

- 493 Chen, Y.B., Seo, S.Y., Kirsch, D.G., Sheu, T.T., Cheng, W.C., Hardwick, J.M., 2006.  
494 Alternate functions of viral regulators of cell death. *Cell Death Differ* 13(8), 1318-1324.
- 495 Collins, J.A., Schandi, C.A., Young, K.K., Vesely, J., Willingham, M.C., 1997. Major DNA  
496 fragmentation is a late event in apoptosis. *J Histochem Cytochem* 45(7), 923-934.
- 497 Dai, J.P., Li, W.Z., Zhao, X.F., Wang, G.F., Yang, J.C., Zhang, L., Chen, X.X., Xu, Y.X., Li,  
498 K.S., 2012. A drug screening method based on the autophagy pathway and studies of the  
499 mechanism of evodiamine against influenza A virus. *PLoS One* 7(8), e42706.
- 500 Dreux, M., Chisari, F.V., 2011. Impact of the autophagy machinery on hepatitis C virus  
501 infection. *Viruses* 3(8), 1342-1357.
- 502 Duriez, P.J., Shah, G.M., 1997. Cleavage of poly(ADP-ribose) polymerase: a sensitive  
503 parameter to study cell death. *Biochem Cell Biol* 75(4), 337-349.
- 504 Edinger, A.L., Thompson, C.B., 2004. Death by design: apoptosis, necrosis and autophagy.  
505 *Curr Opin Cell Biol* 16(6), 663-669.
- 506 Eisenberg-Lerner, A., Bialik, S., Simon, H.U., Kimchi, A., 2009. Life and death partners:  
507 apoptosis, autophagy and the cross-talk between them. *Cell Death Differ* 16(7), 966-975.
- 508 Ekert, P.G., Silke, J., Vaux, D.L., 1999. Caspase inhibitors. *Cell Death Differ* 6(11), 1081-  
509 1086.
- 510 Fernandes-Alnemri, T., Litwack, G., Alnemri, E.S., 1995. Mch2, a new member of the  
511 apoptotic Ced-3/Ice cysteine protease gene family. *Cancer Res* 55(13), 2737-2742.
- 512 Fischer, R., Baumert, T., Blum, H.E., 2007. Hepatitis C virus infection and apoptosis. *World*  
513 *J Gastroenterol* 13(36), 4865-4872.

- 514 Gannage, M., Dormann, D., Albrecht, R., Dengjel, J., Torossi, T., Ramer, P.C., Lee, M.,  
515 Strowig, T., Arrey, F., Conenello, G., Pypaert, M., Andersen, J., Garcia-Sastre, A., Munz,  
516 C., 2009. Matrix protein 2 of influenza A virus blocks autophagosome fusion with  
517 lysosomes. *Cell Host Microbe* 6(4), 367-380.
- 518 Gannage, M., Ramer, P.C., Munz, C., 2010. Targeting Beclin 1 for viral subversion of  
519 macroautophagy. *Autophagy* 6(1), 166-167.
- 520 Garcia-Calvo, M., Peterson, E.P., Leiting, B., Ruel, R., Nicholson, D.W., Thornberry, N.A.,  
521 1998. Inhibition of human caspases by peptide-based and macromolecular inhibitors. *J*  
522 *Biol Chem* 273(49), 32608-32613.
- 523 Germain, M., Affar, E.B., D'Amours, D., Dixit, V.M., Salvesen, G.S., Poirier, G.G., 1999.  
524 Cleavage of automodified poly(ADP-ribose) polymerase during apoptosis. Evidence for  
525 involvement of caspase-7. *J Biol Chem* 274(40), 28379-28384.
- 526 Gonzalez, M.E., Carrasco, L., 2003. Viroporins. *FEBS Lett* 552(1), 28-34.
- 527 Gordy, C., He, Y.W., 2012. The crosstalk between autophagy and apoptosis: where does this  
528 lead? *Protein Cell* 3(1), 17-27.
- 529 Griffin, S.D., Beales, L.P., Clarke, D.S., Worsfold, O., Evans, S.D., Jaeger, J., Harris, M.P.,  
530 Rowlands, D.J., 2003. The p7 protein of hepatitis C virus forms an ion channel that is  
531 blocked by the antiviral drug, Amantadine. *FEBS Lett* 535(1-3), 34-38.
- 532 Griffin, S.D.C., Harvey, R., Clarke, D.S., Barclay, W.S., Harris, M., Rowlands, D.J., 2004. A  
533 conserved basic loop in hepatitis C virus p7 protein is required for amantadine-sensitive  
534 ion channel activity in mammalian cells but is dispensable for localization to  
535 mitochondria. *J Gen Virol* 85, 451-461.



- 536 He, C., Levine, B., 2010. The Beclin 1 interactome. *Curr Opin Cell Biol* 22(2), 140-149.
- 537 Hetz, C.A., Torres, V., Quest, A.F., 2005. Beyond apoptosis: nonapoptotic cell death in  
538 physiology and disease. *Biochem Cell Biol* 83(5), 579-588.
- 539 Kang, R., Zeh, H.J., Lotze, M.T., Tang, D., 2011. The Beclin 1 network regulates autophagy  
540 and apoptosis. *Cell Death Differ* 18(4), 571-580.
- 541 Khaliq, S., Jahan, S., Hassan, S., 2011. Hepatitis C virus p7:molecular function and  
542 importance in hepatitis C virus life cycle and potential antiviral target. *Liver Int* 31(5),  
543 606-617.
- 544 Kim, C.S., Keum, S.J., Jang, S.K., 2011. Generation of a cell culture-adapted hepatitis C  
545 virus with longer half life at physiological temperature. *PLoS One* 6(8), e22808.
- 546 Kumar, S., 2007. Caspase function in programmed cell death. *Cell Death Differ* 14(1), 32-43.
- 547 Lang, F., Lang, K.S., Wieder, T., Myssina, S., Birka, C., Lang, P.A., Kaiser, S., Kempe, D.,  
548 Duranton, C., Huber, S.M., 2003. Cation channels, cell volume and the death of an  
549 erythrocyte. *Pflugers Arch* 447(2), 121-125.
- 550 Liao, Y., Yuan, Q., Torres, J., Tam, J.P., Liu, D.X., 2006. Biochemical and functional  
551 characterization of the membrane association and membrane permeabilizing activity of  
552 the severe acute respiratory syndrome coronavirus envelope protein. *Virology* 349(2),  
553 264-275.
- 554 Lin, C., Lindenbach, B.D., Pragai, B.M., McCourt, D.W., Rice, C.M., 1994. Processing in the  
555 hepatitis C virus E2-NS2 region: identification of p7 and two distinct E2-specific  
556 products with different C termini. *J Virol* 68(8), 5063-5073.

- 557 Lippke, J.A., Gu, Y., Sarnecki, C., Caron, P.R., Su, M.S., 1996. Identification and  
558 characterization of CPP32/Mch2 homolog 1, a novel cysteine protease similar to CPP32.  
559 J Biol Chem 271(4), 1825-1828.
- 560 Madan, V., Castello, A., Carrasco, L., 2008. Viroporins from RNA viruses induce caspase-  
561 dependent apoptosis. Cell Microbiol 10(2), 437-451.
- 562 Malireddi, R.K., Ippagunta, S., Lamkanfi, M., Kanneganti, T.D., 2010. Cutting edge:  
563 proteolytic inactivation of poly(ADP-ribose) polymerase 1 by the Nlrp3 and Nlrc4  
564 inflammasomes. J Immunol 185(6), 3127-3130.
- 565 Mankouri, J., Dallas, M.L., Hughes, M.E., Griffin, S.D., Macdonald, A., Peers, C., Harris, M.,  
566 2009. Suppression of a pro-apoptotic K<sup>+</sup> channel as a mechanism for hepatitis C virus  
567 persistence. Proc Natl Acad Sci U S A 106(37), 15903-15908.
- 568 Mihm, U., Grigorian, N., Welsch, C., Herrmann, E., Kronenberger, B., Teuber, G., von  
569 Wagner, M., Hofmann, W.P., Albrecht, M., Lengauer, T., Zeuzem, S., Sarrazin, C., 2006.  
570 Amino acid variations in hepatitis C virus p7 and sensitivity to antiviral combination  
571 therapy with amantadine in chronic hepatitis C. Antivir Ther 11(4), 507-519.
- 572 Mizushima, N., 2009. Methods for monitoring autophagy using GFP-LC3 transgenic mice.  
573 Methods Enzymol 452, 13-23.
- 574 Montserret, R., Saint, N., Vanbelle, C., Salvay, A.G., Simorre, J.P., Ebel, C., Sapay, N.,  
575 Renisio, J.G., Bockmann, A., Steinmann, E., Pietschmann, T., Dubuisson, J., Chipot, C.,  
576 Penin, F., 2010. NMR structure and ion channel activity of the p7 protein from hepatitis C  
577 virus. J Biol Chem 285(41), 31446-31461.
- 578 Munz, C., 2011. Beclin-1 targeting for viral immune escape. Viruses 3(7), 1166-1178.

- 579 Muzio, M., Chinnaiyan, A.M., Kischkel, F.C., O'Rourke, K., Shevchenko, A., Ni, J., Scaffidi,  
580 C., Bretz, J.D., Zhang, M., Gentz, R., Mann, M., Krammer, P.H., Peter, M.E., Dixit, V.M.,  
581 1996. FLICE, a novel FADD-homologous ICE/CED-3-like protease, is recruited to the  
582 CD95 (Fas/APO-1) death--inducing signaling complex. *Cell* 85(6), 817-827.
- 583 Orth, K., Chinnaiyan, A.M., Garg, M., Froelich, C.J., Dixit, V.M., 1996. The CED-3/ICE-like  
584 protease Mch2 is activated during apoptosis and cleaves the death substrate lamin A. *J*  
585 *Biol Chem* 271(28), 16443-16446.
- 586 Park, J., Kang, W., Ryu, S.W., Kim, W.I., Chang, D.Y., Lee, D.H., Park do, Y., Choi, Y.H.,  
587 Choi, K., Shin, E.C., Choi, C., 2012. Hepatitis C virus infection enhances TNFalpha-  
588 induced cell death via suppression of NF-kappaB. *Hepatology* 56(3), 831-840.
- 589 Pavlovic, D., Neville, D.C., Argaud, O., Blumberg, B., Dwek, R.A., Fischer, W.B., Zitzmann,  
590 N., 2003. The hepatitis C virus p7 protein forms an ion channel that is inhibited by long-  
591 alkyl-chain iminosugar derivatives. *Proc Natl Acad Sci U S A* 100(10), 6104-6108.
- 592 Rasband, W.S., ImageJ. U. S. National Institutes of Health, Bethesda, Maryland, USA, pp.  
593 Accessed from <http://imagej.nih.gov/ij/>, 1999-2012.
- 594 Shrivastava, S., Raychoudhuri, A., Steele, R., Ray, R., Ray, R.B., 2011. Knockdown of  
595 autophagy enhances the innate immune response in hepatitis C virus-infected hepatocytes.  
596 *Hepatology* 53(2), 406-414.
- 597 Simmonds, P., 2004. Genetic diversity and evolution of hepatitis C virus--15 years on. *J Gen*  
598 *Virol* 85(Pt 11), 3173-3188.

- 599 Soo, H.M., Garzino-Demo, A., Hong, W., Tan, Y.H., Tan, Y.J., Goh, P.Y., Lim, S.G., Lim,  
600 S.P., 2002. Expression of a full-length hepatitis C virus cDNA up-regulates the  
601 expression of CC chemokines MCP-1 and RANTES. *Virology* 303(2), 253-277.
- 602 Steinmann, E., Penin, F., Kallis, S., Patel, A.H., Bartenschlager, R., Pietschmann, T., 2007.  
603 Hepatitis C virus p7 protein is crucial for assembly and release of infectious virions.  
604 *PLoS Pathog* 3(7), e103.
- 605 Steinmann, E., Pietschmann, T., 2010. Hepatitis C Virus P7-A Viroporin Crucial for Virus  
606 Assembly and an Emerging Target for Antiviral Therapy. *Viruses-Basel* 2(9), 2078-2095.
- 607 StGelais, C., Foster, T.L., Verow, M., Atkins, E., Fishwick, C.W., Rowlands, D., Harris, M.,  
608 Griffin, S., 2009. Determinants of hepatitis C virus p7 ion channel function and drug  
609 sensitivity identified in vitro. *J Virol* 83(16), 7970-7981.
- 610 Szabo, I., Adams, C., Gulbins, E., 2004. Ion channels and membrane rafts in apoptosis.  
611 *Pflugers Arch* 448(3), 304-312.
- 612 Taguwa, S., Kambara, H., Fujita, N., Noda, T., Yoshimori, T., Koike, K., Moriishi, K.,  
613 Matsuura, Y., 2011. Dysfunction of autophagy participates in vacuole formation and cell  
614 death in cells replicating hepatitis C virus. *J Virol* 85(24), 13185-13194.
- 615 Tan, Y.X., Tan, T.H., Lee, M.J., Tham, P.Y., Gunalan, V., Druce, J., Birch, C., Catton, M.,  
616 Fu, N.Y., Yu, V.C., Tan, Y.J., 2007. Induction of apoptosis by the severe acute  
617 respiratory syndrome coronavirus 7a protein is dependent on its interaction with the Bcl-  
618 XL protein. *J Virol* 81(12), 6346-6355.

- 619 Tedbury, P., Welbourn, S., Pause, A., King, B., Griffin, S., Harris, M., 2011. The subcellular  
620 localization of the hepatitis C virus non-structural protein NS2 is regulated by an ion  
621 channel-independent function of the p7 protein. *J Gen Virol* 92, 819-830.
- 622 Tewari, M., Quan, L.T., O'Rourke, K., Desnoyers, S., Zeng, Z., Beidler, D.R., Poirier, G.G.,  
623 Salvesen, G.S., Dixit, V.M., 1995. Yama/CPP32 beta, a mammalian homolog of CED-3,  
624 is a CrmA-inhibitable protease that cleaves the death substrate poly(ADP-ribose)  
625 polymerase. *Cell* 81(5), 801-809.
- 626 Wakita, T., Pietschmann, T., Kato, T., Date, T., Miyamoto, M., Zhao, Z., Murthy, K.,  
627 Habermann, A., Krausslich, H.G., Mizokami, M., Bartenschlager, R., Liang, T.J., 2005.  
628 Production of infectious hepatitis C virus in tissue culture from a cloned viral genome.  
629 *Nat Med* 11(7), 791-796.
- 630 WHO, 2012. Hepatitis C. Fact sheet N°164, July 2012 ed. World Health Organization.
- 631 Xiao, J.H., Davidson, I., Matthes, H., Garnier, J.M., Chambon, P., 1991. Cloning, expression,  
632 and transcriptional properties of the human enhancer factor TEF-1. *Cell* 65(4), 551-568.
- 633 Yang, Y., Zhao, S., Song, J., 2004. Caspase-dependent apoptosis and -independent  
634 poly(ADP-ribose) polymerase cleavage induced by transforming growth factor beta1. *Int*  
635 *J Biochem Cell Biol* 36(2), 223-234.
- 636 Zhou, F., Yang, Y., Xing, D., 2011. Bcl-2 and Bcl-xL play important roles in the crosstalk  
637 between autophagy and apoptosis. *FEBS J* 278(3), 403-413.
- 638
- 639
- 640
- 641

**642 Figure legends**

643 *Fig. 1.* Induction of apoptosis by overexpression of HCV genotype 1b (S1) and genotype 2a  
644 p7 in Huh7.5 cells. (A) Apo-One fluorometric assay system from Promega Corporation  
645 (Madison, WI) was used to measure the activation of caspase-3/7, which is a hallmark of  
646 apoptosis, in Huh7.5 cells that were transfected with empty vector, p7 of genotype 1b (p7-1b),  
647 p7 of genotype 2a (p7-2a) and Bax. All experiments were performed in triplicate, and the  
648 average values with standard deviations are plotted. (B) Western blot analysis was performed  
649 to determine the expression levels of the flag-tagged proteins in the different samples used in  
650 (A) (top), the cleavage of endogenous PARP (middle), and the levels of endogenous actin as  
651 a loading control of total cell lysates used (bottom). *P-values* indicated by asterisks are  
652 considered statistically significant,  $p < 0.01$  (\*).

653

654

655 *Fig. 2.* HCV p7 induces apoptosis via caspase-dependent pathways. (A) Apo-One  
656 fluorometric assay system from Promega Corporation (Madison, WI) was used to measure  
657 the activation of caspase-3/7 in Huh7.5 cells that were transfected with empty vector or flag-  
658 tagged p7. The cells were treated with an irrelevant peptide, zFA-fmk (columns 1 and 2) or a  
659 pan-caspase inhibitor, zVAD-fmk (columns 3 and 4). All experiments were performed in  
660 triplicate, and the average values with standard deviations are plotted. (B) Western blot  
661 analysis was performed to determine the expression levels of the flag-tagged proteins in the  
662 different samples used in (A) (top), the cleavage of endogenous PARP (middle), and the  
663 levels of endogenous actin as a loading control of total cell lysates used (bottom). Percentage  
664 cleaved-PARP values are shown below the blots. *P-values* indicated by asterisks are  
665 considered statistically significant,  $p < 0.01$  (\*).

666

667 *Fig. 3.* HCV p7 induced apoptosis is via both the intrinsic and extrinsic apoptosis pathways.  
668 (A) Apo-One fluorometric assay system from Promega Corporation (Madison, WI) was used  
669 to measure the activation of caspase-3/7 in Huh7.5 cells that were transiently transfected with  
670 empty vector or flag-tagged p7. The cells were treated with an irrelevant peptide (zFA-fmk)  
671 or caspase-3, caspase-8 and caspase-9 inhibitors (zDEVD-fmk, zIETD-fmk and zLEHD-fmk).  
672 All experiments were performed in triplicate, and the average values with standard deviations  
673 are plotted. (B) Western blot analysis was performed to determine the expression levels of the  
674 flag-tagged proteins in the different samples used in (A) (top), the cleavage of endogenous  
675 PARP (middle), and the levels of endogenous actin as a loading control of total cell lysates  
676 used (bottom). *P-values* indicated by asterisks are considered statistically significant,  $p <$   
677  $0.01$  (\*).

678

679

680 *Fig. 4.* Detection of HCV p7 induced apoptotic cell by TUNEL assay. The DeadEnd™  
681 Fluorometric TUNEL System from Promega Corporation (Madison, WI) was used to  
682 measure the activation of caspase-3/7 in Huh7.5 cells that were transiently transfected with  
683 empty vector or flag-tagged p7. The cells were treated with an irrelevant peptide (zFA-fmk)  
684 or caspase-3, caspase-8 and caspase-9 inhibitors (zDEVD-fmk, zIETD-fmk and zLEHD-fmk).  
685 At 24 h post transfection, the cells were fixed and permeabilized, and TUNEL assay was  
686 performed.

687

688 *Fig. 5.* HCV p7 induced apoptosis is independent of its ion channel activity. (A) Modification  
689 of membrane permeability by HCV p7 protein. 293FT cells expressing wild-type p7 protein  
690 or the mutant (p7H17A31A) were treated with 0, 1, and 2 mM of hygromycin B for 30 min at  
691 6 h post-transfection (lanes 1, 2, and 3). Cell lysates were prepared and the expression of the

692 flag-tagged proteins was detected by immunoprecipitation with anti-Flag antibody under mild  
693 washing conditions. Proteins were separated by SDS-PAGE and visualized by  
694 autoradiography. The percentages of p7 and p7H17AH31A proteins detected in the presence  
695 of hygromycin B were determined by densitometry and indicated at the bottom. (B) Apo-One  
696 fluorometric assay system from Promega Corporation was used to measure the activation of  
697 caspase-3/7 in Huh7.5 cells 24 hours post-transfection with flag-vector, wild-type p7,  
698 p7H17AH31A substitution mutant and the known apoptosis inducer, Bax. (B) Western blot  
699 analysis was performed to determine the expression levels of the different flag-tagged  
700 proteins (top) and the cleavage of endogenous PARP, which is a substrate of activated  
701 caspase-3, from 116 to 83 kDa (middle). Equal sample loading was verified by the detection  
702 of endogenous actin (bottom). *P-values* indicated by asterisks are considered statistically  
703 significant,  $p < 0.01$  (\*).

704

705

706 *Fig. 6.* HCV p7 induced apoptosis is dependent on the cellular topology of p7 protein. (A)  
707 Apo-One fluorometric assay system from Promega Corporation was used to measure the  
708 activation of caspase-3/7 in Huh7.5 cells 24 hours post-transfection with flag-vector, wild-  
709 type p7, substitution mutants (containing either R to A or changes) and the known apoptosis  
710 inducer, Bax. (B) Western blot analysis was performed to determine the expression levels of  
711 the different flag-tagged proteins (top) and the cleavage of endogenous PARP, which is a  
712 substrate of activated caspase-3, from 116 to 83 kDa (middle). Equal sample loading was  
713 verified by the detection of endogenous actin (bottom). *P-values* indicated by asterisks are  
714 considered statistically significant,  $p < 0.01$  (\*).

715



716 *Fig. 7.* HCV p7 induces a higher level of apoptosis than M2 of influenza A virus. (A) Apo-  
717 One fluorometric assay system from Promega Corporation was used to measure the activation  
718 of caspase-3/7 in 293FT cells 24 hours post-transfection with flag-vector, flag-p7, flag-M2  
719 and the known apoptosis inducer, Bax. (B) Western blot analysis was performed to  
720 determine the expression levels of the different flag-tagged proteins (top) and the cleavage of  
721 endogenous PARP, which is a substrate of activated caspase-3/7 (middle). Equal sample  
722 loading was verified by the detection of endogenous actin (bottom). The multiple bands  
723 (indicated by  $\alpha$ ) in lane 2 are oligomers of M2. *P-values* indicated by asterisks are considered  
724 statistically significant,  $p < 0.01$  (\*).

725

726

727 *Fig. 8.* HCV p7 does not induce accumulation of autophagosomes. (A) Measurement of the  
728 conversion of LC3-I to LC3-II was used as an autophagic marker. 293FT cells, mock  
729 transfected, or transiently transfected with flag vector, flag p7, flag-M2 and untransfected  
730 cells untreated or treated with ammonium chloride were analysed by Western blot analysis  
731 using anti-LC3 antibody (middle). Similarly, the expression levels of the different flag-tagged  
732 proteins were determined (top). Equal sample loading was verified by the detection of  
733 endogenous actin (bottom). The percentage conversion of LC3-I to LC3-II (i.e. LC3-II/LC3-  
734 I+LC3-II) is calculated after densitometry was used to quantify the intensities of LC3-I and II  
735 in the autoradiographs. Percentage LC3-II values are shown below the blots. (B) The mean  
736 LC3-II values quantified for four independent experiments were computed after densitometry  
737 and are plotted with standard deviations (error bars). *P-values* indicated by asterisks are  
738 considered statistically significant,  $p < 0.05$  (\*\*),  $p < 0.01$  (\*) and no significant difference  
739 (ns).

740

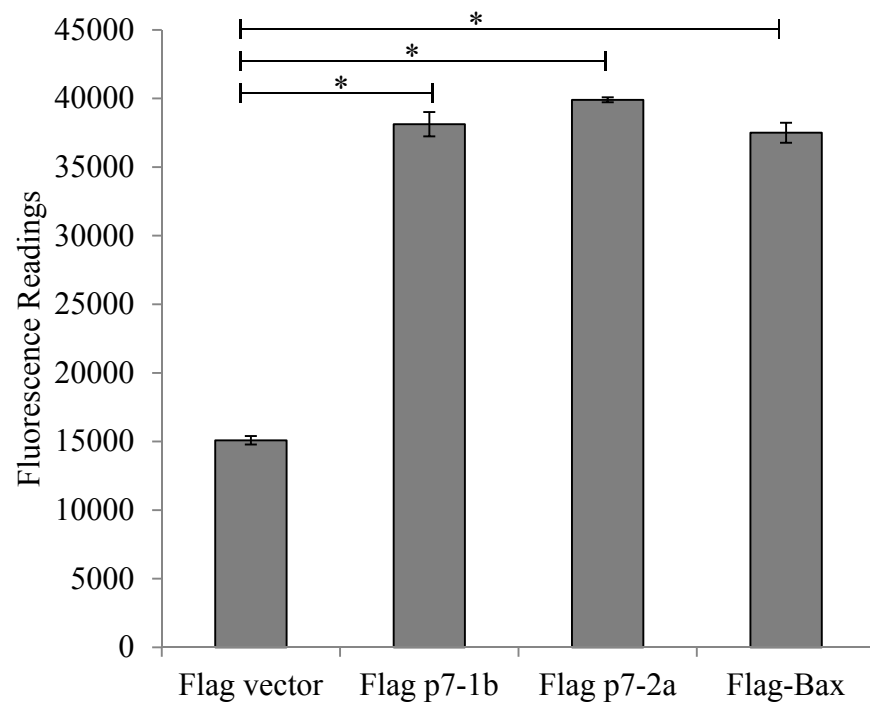
741 *Fig. 9.* Interaction of M2 and p7 proteins with endogenous Beclin-1 and their effects on the  
742 accumulation of GFP-LC3 puncta. (A) Immunofluorescence analysis was performed on  
743 293FT cells transfected with FLAG-tagged GFP-LC3 and expression plasmids encoding  
744 either FLAG-tagged M2 or p7. Twenty-four hours after transfection, cells expressing GFP-  
745 LC3 (green) and p7 or M2 (red) were analyzed by fluorescence microscopy. Merged images  
746 are shown below. (B) Co-immunoprecipitation of M2 and p7 proteins with endogenous  
747 Beclin-1. 293FT cells were transfected with flag-vector, flag-GST (negative control), flag-  
748 M2 and flag-p7. The cells were harvested at about 24 h post-transfection, lysed, and  
749 subjected to IP with anti-Beclin-1 antibody and protein A agarose beads. The amount of flag-  
750 tagged proteins that co-immunoprecipitated (IP) with Beclin-1 was determined by Western  
751 blot analysis (WB) with an anti-flag antibody (top). The amounts of flag-tagged proteins and  
752 endogenous Beclin-1 in the lysates before IP were determined by subjecting aliquots of the  
753 lysates to Western blot analysis (middle and bottom). The protein marked with Greek letter  
754 beta ( $\beta$ ) represents the heavy chain of the antibody used for IP.

755

756

Fig. 1

A



B

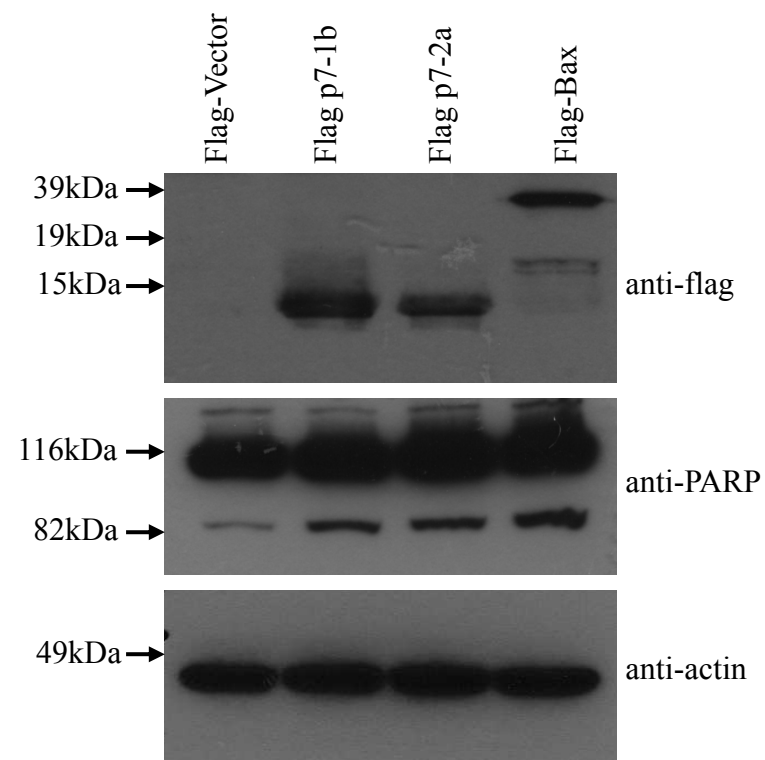


Fig. 2

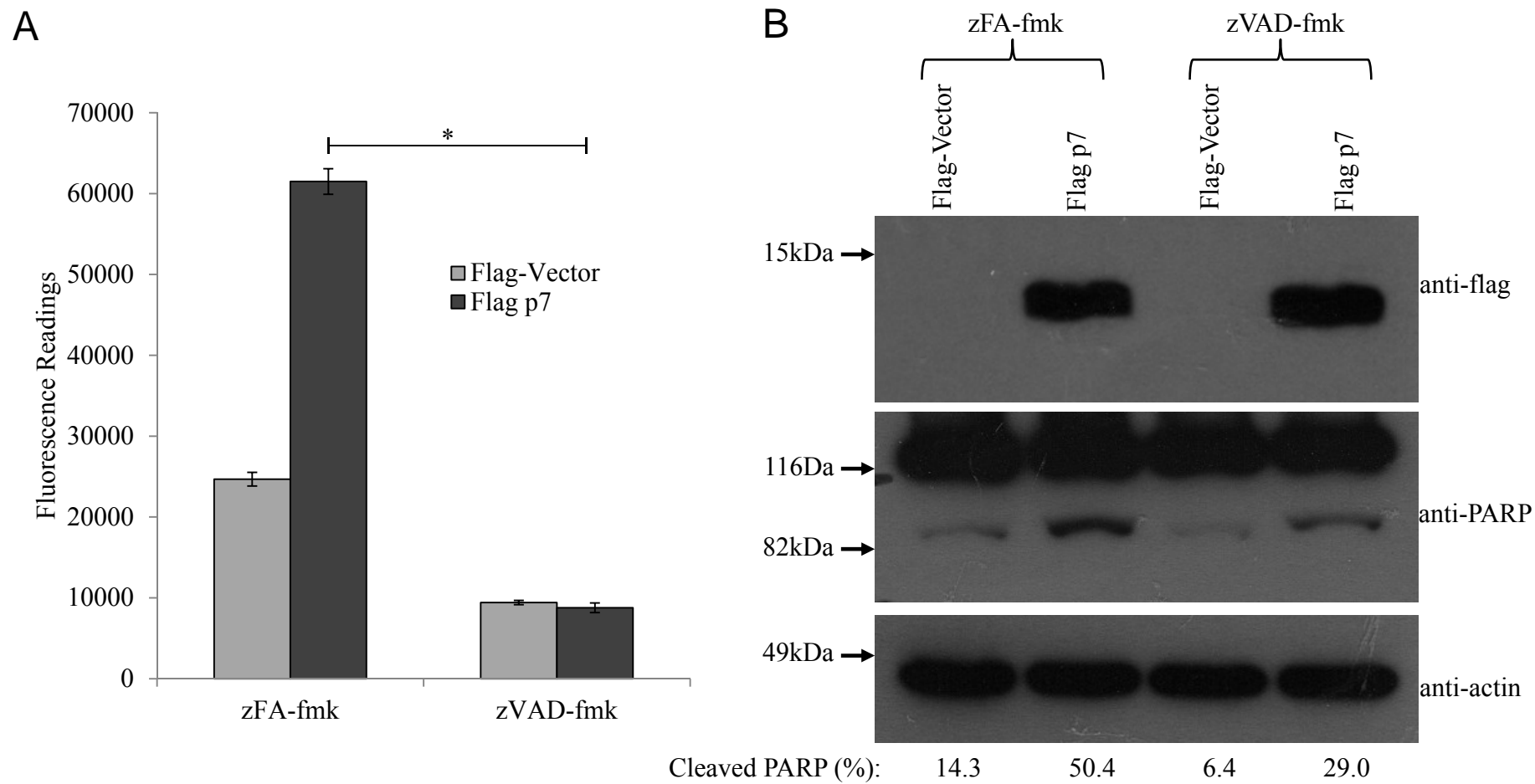




Fig. 4

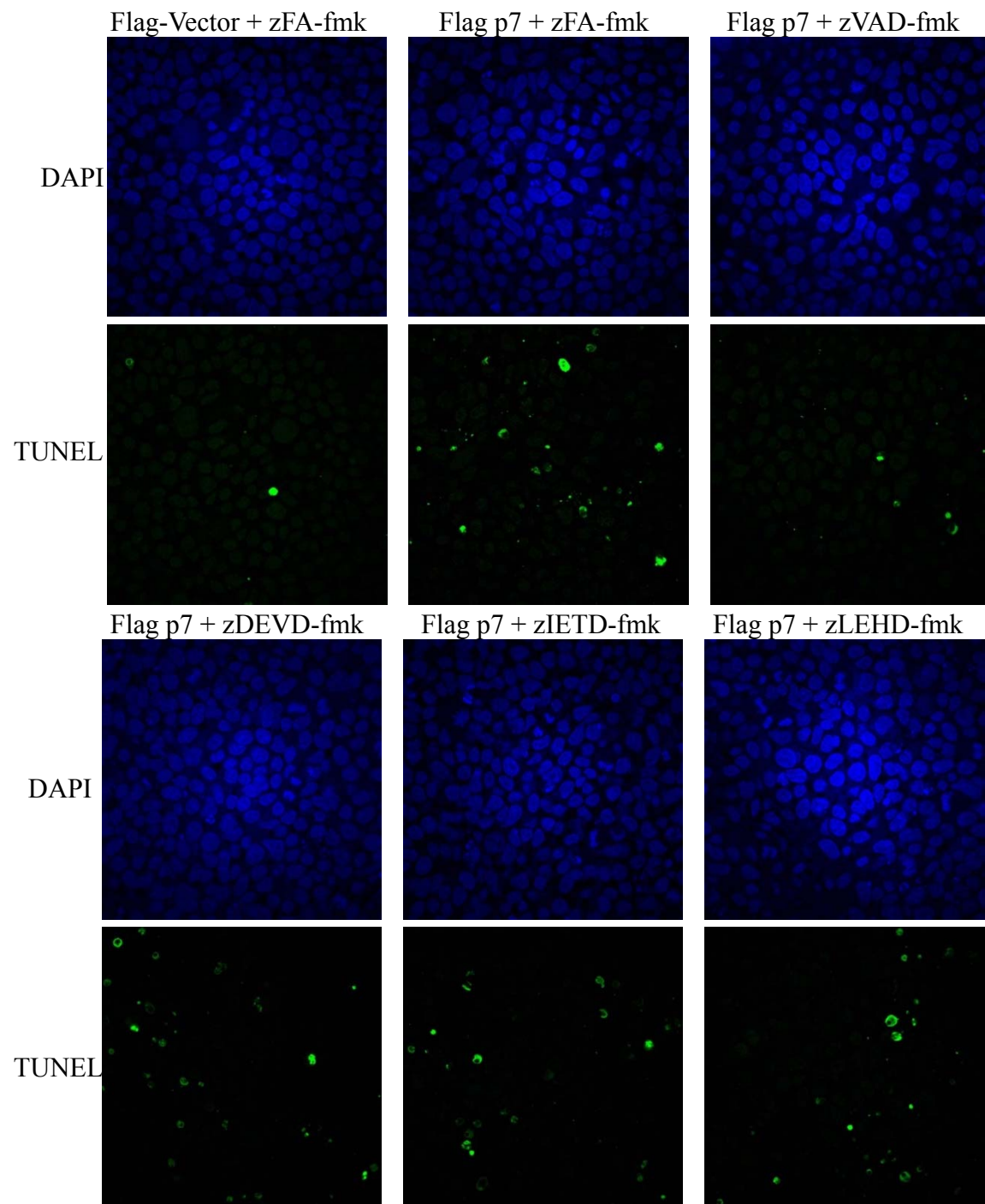
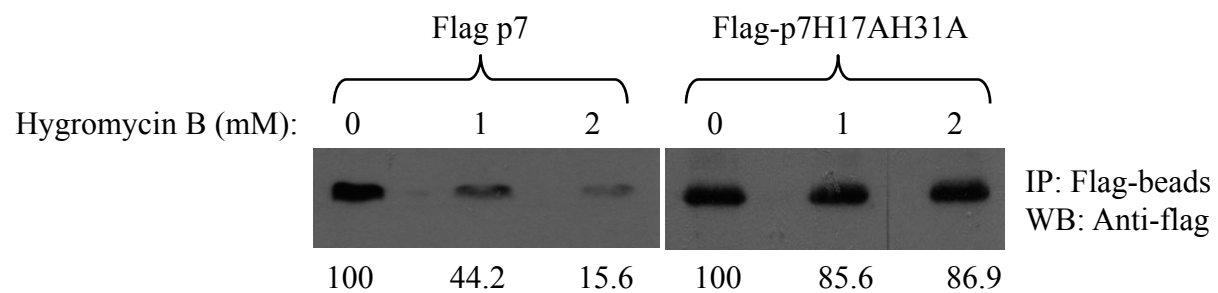
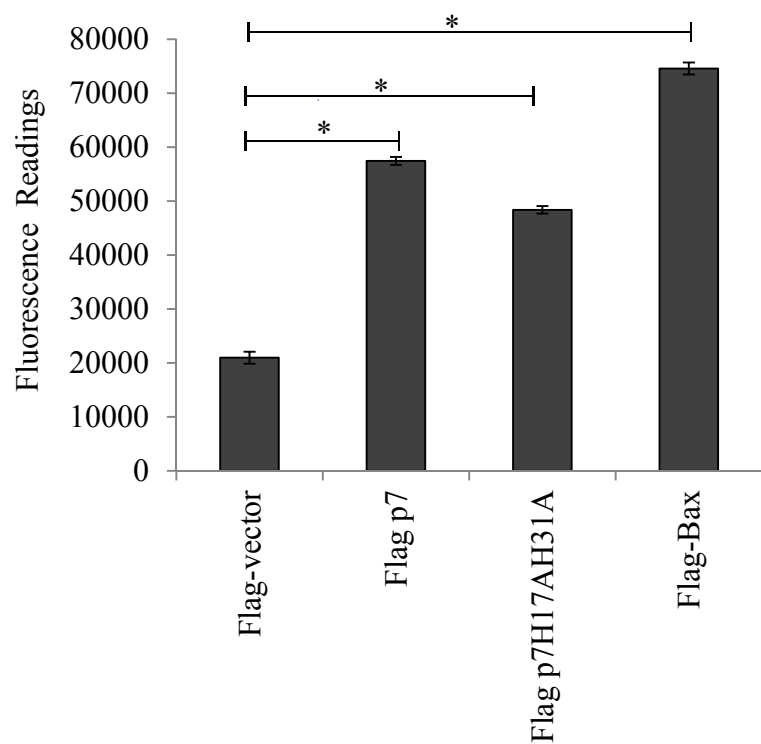


Fig. 5

A



B



C

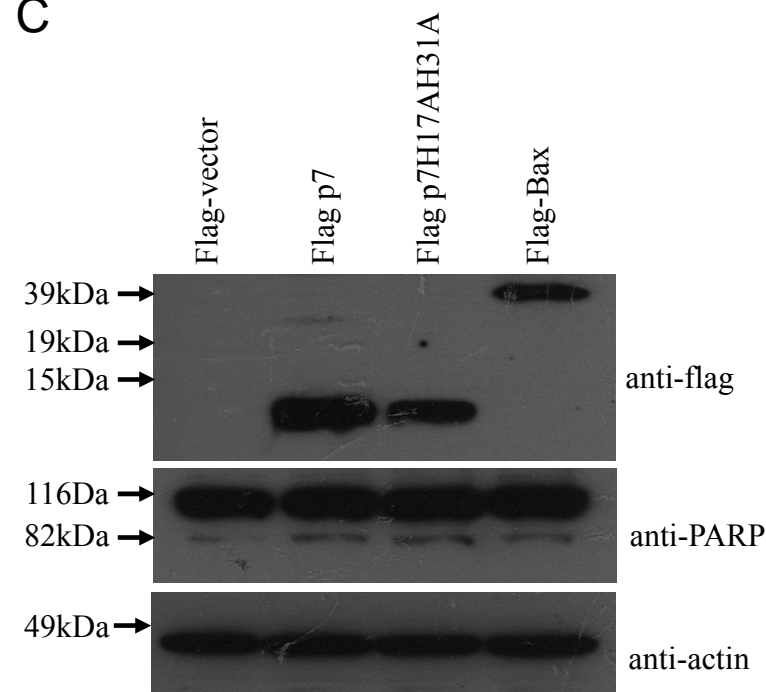
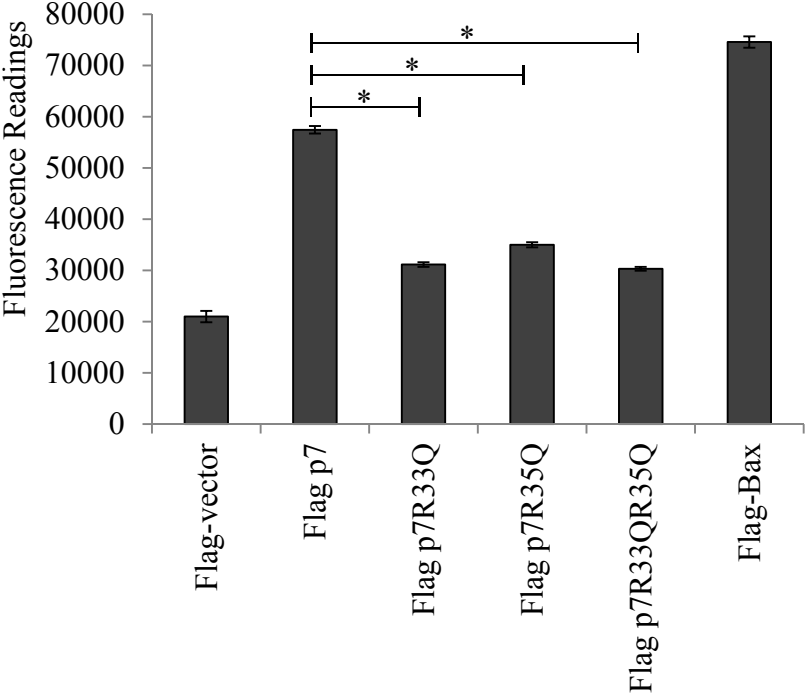


Fig. 6

A



B

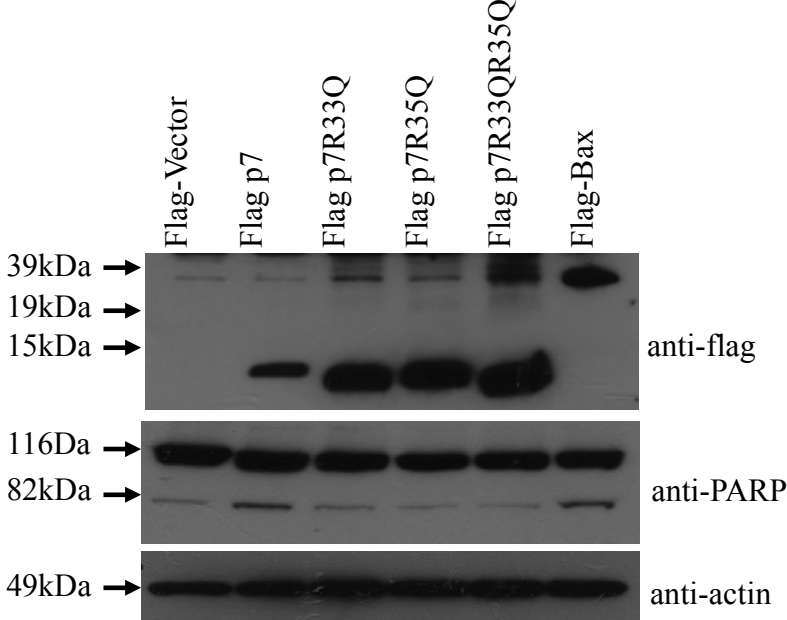
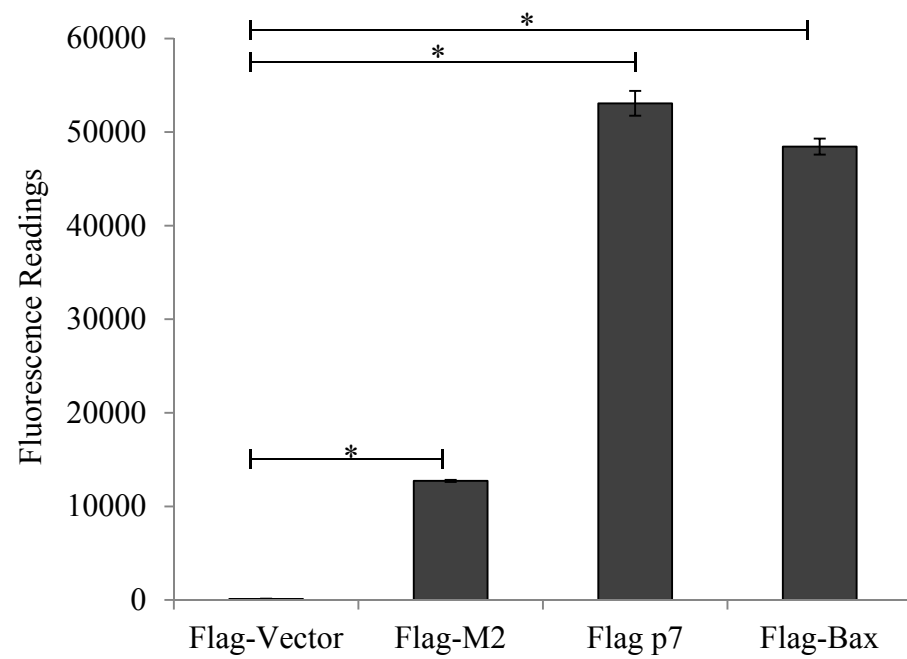




Fig. 7

A



B

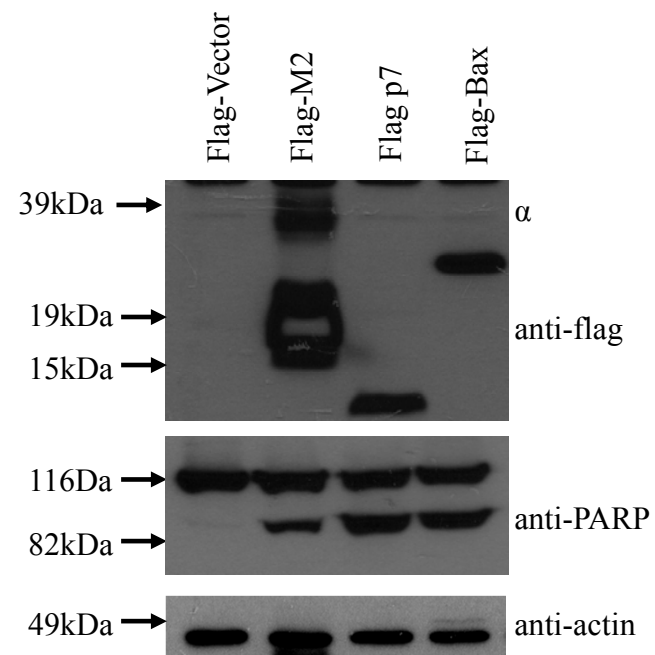
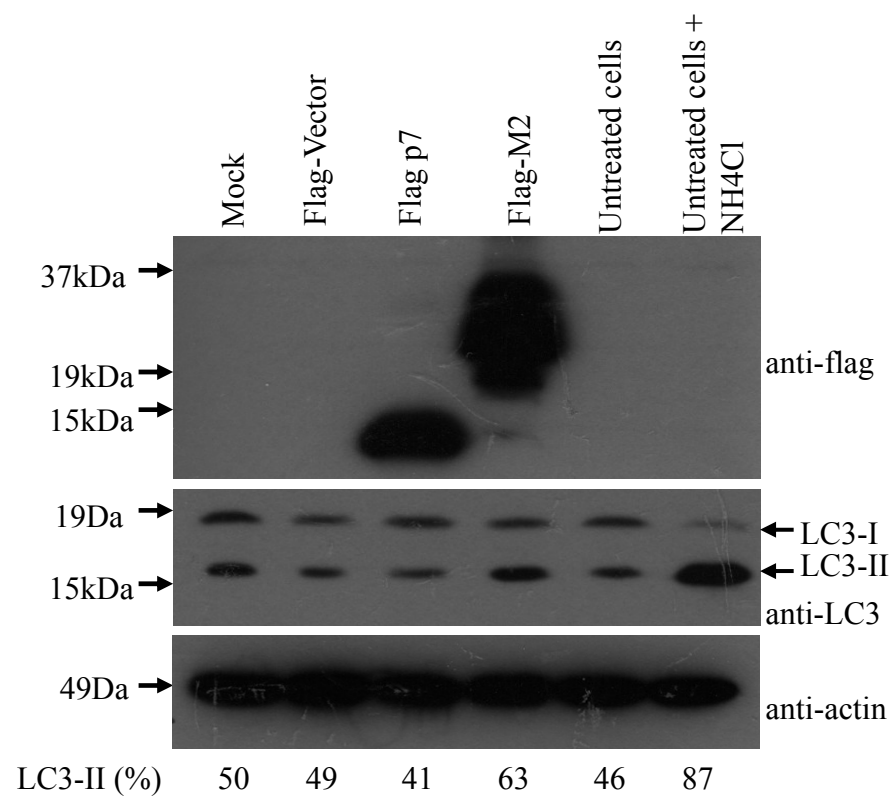


Fig. 8

A



B

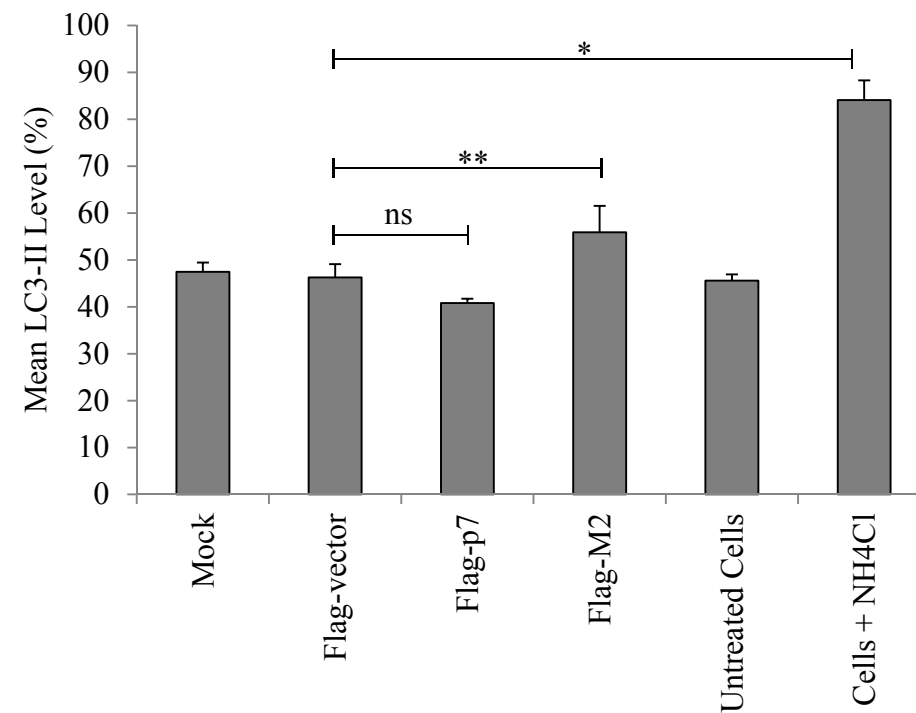
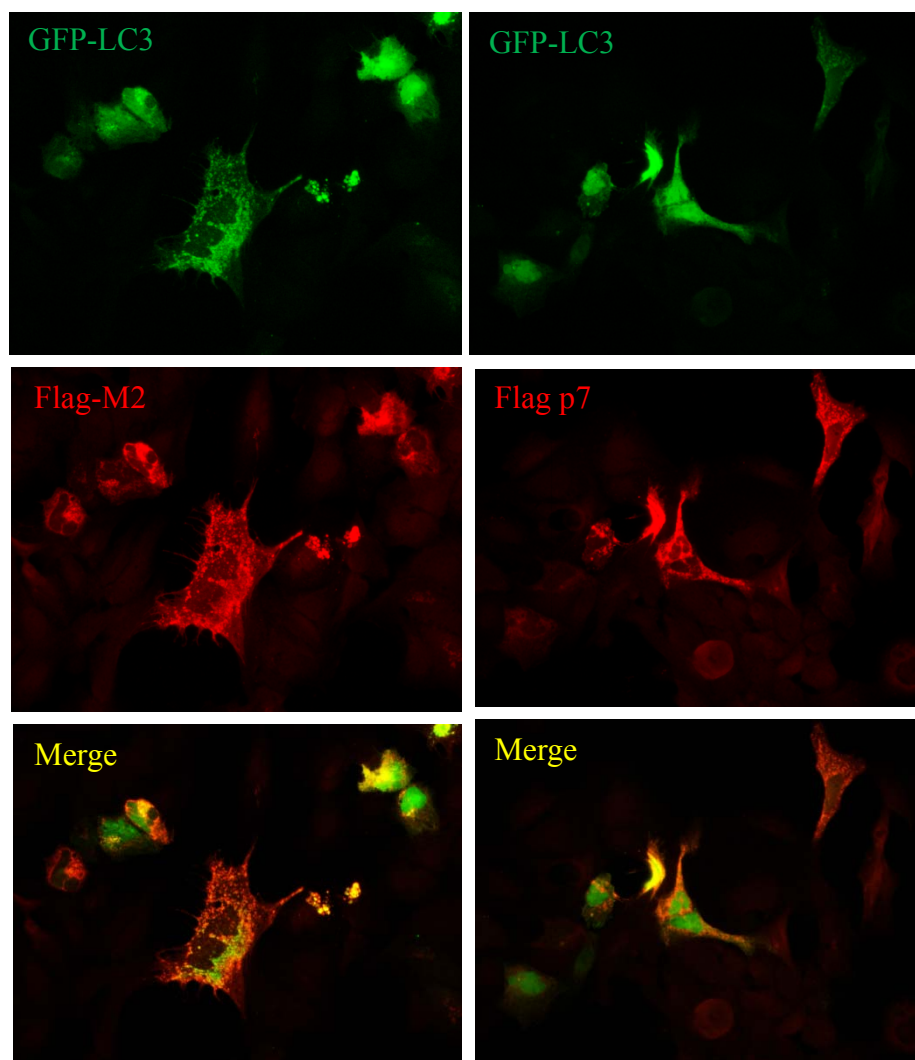


Fig. 9

A



B

